An optimisation model of the diel vertical migration of northern krill (*Meganyctiphanes norvegica*) in the Clyde Sea and the Kattegat

Geraint Tarling, Michael Burrows, Jack Matthews, Reinhard Saborowski, Friedrich Buchholz, Alain Bedo, and Patrick Mayzaud

Abstract: An optimisation model was developed to examine the effect of predation risk and environmental conditions on the diel vertical migration (DVM) of adult northern krill (*Meganyctiphanes norvegica*). Model predictions were compared in two locations with contrasting environmental conditions, the Clyde Sea and the Kattegat. The model was constructed from a combination of parameterised functions and empirical field data obtained during summer conditions. Parameter matrices were set up to cover the entire water column over a 24-h period. The first matrix contained values for "net energy gain," which incorporated empirical data on temperature-dependent respiration, copepod and phytoplankton abundance, and a functional response model for feeding rate. The second matrix expressed the risk of encountering a generalised visual (fish) predator as a function of light levels. The optimisation procedure sought a path through depth and time such that the energy gain was equal to the amount necessary to grow, produce eggs, and moult, while the risk of predation was minimised. The model predicted DVM in both the Clyde Sea and the Kattegat. Sensitivity analyses showed that the predicted DVM pattern was mainly driven by food and predation risk, with temperature effects on metabolic costs having a minor effect.

Résumé : Nous avons élaboré un modèle d'optimisation pour examiner les effets du risque de prédation et des conditions environnementales sur la migration verticale nycthémérale du krill nordique (*Meganyctiphanes norvegica*) adulte. Les prédictions du modèle ont été comparées à deux endroits présentant des conditions environnementales très différentes, la mer de Clyde et le Kattegat. Le modèle a été construit à partir d'une combinaison de fonctions paramétrisées et de données empiriques de terrain obtenues dans des conditions estivales. Les matrices des paramètres ont été établies de façon à couvrir l'ensemble de la colonne d'eau sur une période de 24 h. La première matrice contenait des valeurs correspondant au « gain énergétique net » qui intégraient les données empiriques sur la respiration dépendante de la température, l'abondance des copépodes et du phytoplancton et un modèle de réaction fonctionnelle pour le taux d'alimentation. La deuxième matrice exprimait le risque de rencontrer un prédateur visuellement généralisé (poisson) en fonction du niveau d'éclairement. La procédure d'optimisation a formulé un cheminement dans la profondeur et dans le temps de façon que le gain énergétique soit égal à la quantité nécessaire pour la croissance, la production d'oeufs et la mue, tandis que le risque de prédation était minimisé. Le modèle a prédit la migration verticale nycthémérale en mer de Clyde et dans le Kattegat. Des analyses de sensibilité ont montré que le patron de migration prédit était essentiellement régi par l'alimentation et le risque de prédation, les effets de la température sur les coûts métaboliques n'ayant qu'un effet mineur.

Introduction

Diel vertical migration (DVM) behaviour is a regular pattern of behaviour that is widespread in the zooplankton community, occurring in all oceans at both high and low latitudes (Longhurst 1976). The pattern of migration mainly varies between a normal DVM, where animals ascend to the upper layers at nighttime and descend to deeper layers during the day, and reverse DVM, where ascent is during daytime and descent during the night. Midnight sinking is a commonly observed phenomenon (Tarling et al. 1999 and references therein) where individuals that have migrated to the surface during the evening sink down slowly during the course of the night. There are also many zooplankton spe-

Received February 5, 2000. Accepted June 21, 2000.
J15582

G.A. Tarling[1] and J.B.L Matthews. Scottish Association for Marine Science, P.O. Box 3, Oban, Argyll, PA34 4AD, U.K.
M.T. Burrows. Dunstaffnage Marine Laboratory, P.O. Box 3, Oban, Argyll, PA34 4AD, U.K.
R. Saborowski and F. Buchholz. Biologische Anstalt Helgoland, AWI, Meeresstation, Postfach 180, D-27483 Helgoland, Germany.
A. Bedo and P. Mayzaud. Observatoire Océanologique, UPMC CNRS INSU LOBEPM, Océanographie biochimique et Ecologie, B.P. 28, F-06230, Villefranche sur mer, France.

[1]Author to whom all correspondence should be addressed. e-mail: gant@dml.ac.uk

cies that do not show any type of vertical migration behaviour as well as others in which vertical migration becomes increasingly pronounced during the course of the life cycle (see review by Angel 1985).

Many theories have been put forward as to the cause of vertical migration. One of the earliest postulated that vertical migration afforded escape from predation (Russell 1927). This has been elegantly demonstrated by more recent work that found that species performing the behaviour were more successful in situations where visual fish predators were introduced into lakes (e.g., Zaret and Suffern 1976). This is supported by marine examples where DVM was more apparent during periods when the abundance of visual fish predators was seasonally high (e.g., Bollens and Frost 1989). Field evidence that food concentration influences DVM is not as strong, although the laboratory studies of Johnson and Jakobsen (1987) on *Daphnia longispina* and Huntley and Brooks (1982) on *Calanus pacifica* demonstrated that the behaviour may be modified or even stopped under certain food conditions. The clear relationship between respiration rate and temperature (see Ikeda 1985) suggests an adaptive value in moving up and down vertical temperature gradients in order to gain maximum metabolic advantage (McLaren 1963), although this is contested by more recent modelling studies (e.g., Ohman 1990).

Behavioural strategies that maximise fitness often involve trade-offs (Krebs and Davies 1991), and it has been shown in numerous studies that animals sacrifice food intake in the face of potential danger (e.g., Gilliam and Fraser 1987). With respect to the vertical positioning of zooplankton, this trade-off will vary through a diel cycle as changing light levels alter predator capture ability and prey vulnerability (Mangel and Clark 1988). For modelling purposes, it is necessary to consider such a trade-off quantitatively so that the fitness consequences of foraging and danger can be assessed. The approach taken in this investigation follows that of Gilliam and Fraser (1987) where a forager chooses patches with the lowest ratio of mortality rate to feeding rate subject to the constraint that the feeding rate is above the level required to survive. The advantage of the approach is in its use of ratios that allow application to situations where an absolute quantitative assessment of certain environmental parameters may not be possible. This is because optimal habitats are decided by the general rule

(1) Prefer habitat A to B if: $E_A / E_B < H_A / H_B$

where E is predation risk and H is energy gain, such that the rule depends only on the relative level of mortality and intake in the two sites, not on the absolute levels.

The euphausiid northern krill (*Meganyctiphanes norvegica*) exhibits a pronounced DVM throughout its wide geographical range, which includes the North Atlantic and Arctic oceans and Mediterranean Sea. It feeds on a combination of phytoplankton and copepods depending on their seasonal availability (Mauchline 1960) and is a major part of the diets of pelagic fish such as herring and bottom-dwelling fish such as cod (Tanasichuck 1999). Its wide range of habitats results in separated populations that appear to be adapted to quite contrasting sets of abiotic and biotic conditions. The optimal DVM strategy in such contrasting situations may differ considerably. Comparing predicted DVM patterns against those observed in the field for locations with contrasting environmental conditions is therefore a powerful validation procedure and a good test of the robustness of the model's design.

Northern krill populations in the Clyde Sea and the Kattegat were sites of a major recent investigation (PEP programme; see Acknowledgements and Buchholz et al. 1998) where information was collected on the trophic environment and hydrographic conditions as well as the vertical migration behaviour, respiration rate, and feeding behaviour of northern krill in summer environmental conditions. It was apparent that environmental conditions did differ between the two sites, as did the exact pattern of vertical migration. Through running the model with these different sets of parameter values, the aim was twofold. Firstly, it was to determine whether the model was robust and able to predict a DVM pattern that was close to field observations in contrasting environments. Secondly, it was envisaged that the comparison of the sites, as well as further sensitivity analyses, would identify those parameters that were of greatest importance to producing the predicted patterns.

Material and methods

Structure of the model

The model predicts the vertical migration behaviour of krill over a 24-h period in a summer situation. The water column is divided into intervals of between 10 and 20 m (j) and time into hourly periods (i). A parameter matrix of the energy gain (H) of occupying each of these depth–time cells is calculated by taking away the respiration costs (M_{ij}) of occupying the cell from the expected food intake (F_{ij}) (i.e., $H = I - M$) to give a give a matrix of the form $\{H_{ij}\}$. Correspondingly, a mortality risk matrix of the form $\{E_{ij}\}$ is calculated as a function of light and the visual range of the predator. The model is run iteratively to find a vertical distribution pattern that minimises the total mortality risk over the 24-h period while gaining enough energy to meet the daily demands of growth, moulting, and reproduction. Symbols, definitions, and units for all parameters used in the model are given in Table 1.

Parameters for calculating energy gain (H)

Respiration rate

Respiration rate (M) may be parameterised as a function of temperature and weight in the general form

(2) $$M = aW^b$$

where a is a scaling coefficient, b is the weight-specific exponent for respiration, and W is weight (for zooplankton examples, see Ikeda and Motoda 1978). Stuart (1986) estimated the weight exponent b as 0.845. Temperature dependence of krill respiration was investigated in onboard experiments carried out on the R/V *Heincke* during visits to the Clyde Sea and the Kattegat (Saborowski et al. 2000). Results were combined with those of Stuart (1986) to give the following equation for the hourly respiration rate:

(3) $$M = 0.020334(0.4389 + 0.08938T)W^{0.845}$$

where M is respiration rate and W is dry weight (DW). This was converted to energy assuming that 1 L O_2 respired = 20332 J (Winberg 1971).

Table 1. Symbols, definitions, and units for the parameters used in the model.

Symbol	Definition	Units	Value
j	Depth zone	m	
i	Time interval	h	
H_{ij}	Hourly energy gain	J·h^{-1}	
H_t	Daily energy gain	J·day^{-1}	
M, M_{ij}	Respiration rate	µL O_2·h^{-1}	
F	Expected food intake	µg DW·h^{-1}	
E_{ij}	Mortality risk		
a	Scaling coefficient dependent on temperature	µL O_2·mg^{-1}·h^{-1}	
b	Weight-specific exponent for respiration		
W	Weight (DW)	mg	
T	Temperature	°C	
G	Copepod ingestion rate	µg DW·h^{-1}	
C	Copepod biomass	µg DW·L^{-1}	
P	Proportion of phytoplankton to total energy intake		
Chl *a*	Concentration of Chl *a* in the environment	mg·L^{-1}	
S	Assimilation efficiency		0.8
e	Encounter rate	h^{-1}	
v	Fish velocity	m·h^{-1}	50
N	Fish density	Individuals·m^{-3}	
dt	Time interval	1 h	
θ	Field of view (upward-looking fish)		0.5
r	Visual range	m	
z	Depth	m	
c_z	Local beam attenuation coefficient	m^{-1}	
K	Local diffuse attenuation coefficient	m^{-1}	
ρ	Light fraction lost at the surface		0.5
I_s	Irradiance at the surface	µmol·m^{-2}·s^{-1}	
C_0	Inherent contrast of krill		0.5
A_{zp}	Krill cross-sectional area	m^2	0.0000126
ΔS_e	Sensitivity of planktivore eye	µmol·m^{-2}·s^{-1}	3.0 ×10^{-6}

Ingestion rate: copepods

A copepod ingestion rate equation was developed from the works of McClatchie (1985) and Båmstedt and Karlson (1998). McClatchie (1985) incubated Northern krill in copepod concentrations ranging from 200 to 4000 µg DW·L^{-1} and calculated a functional response curve for the hourly ingestion rate of copepods (G):

$$\log_{10}G = 0.746\log_{10}C - 0.686 \quad (4)$$

where C is copepod biomass. McClatchie (1985) predicted that relatively high concentrations of copepods were necessary (2265 µg DW·L^{-1}) to meet metabolic demands. Båmstedt and Karlson (1998) found that much lower concentrations of copepods were adequate (145 µg DW·L^{-1}). The major difference between the two studies was the size of the incubation chambers (4 L in the former study and 45–90 L in the latter), with the larger chambers used by Båmstedt and Karlson (1998) making them less likely to suppress ingestion rates compared with the McClatchie (1985) study. However, Båmstedt and Karlson (1998) did not expose krill to different concentrations of copepods in order to calculate a functional response curve. Here, we make the assumption that the suppression of ingestion was constant at all concentrations of copepods and adopt the functional response curve of McClatchie (1985). The y intercept of McClatchie's (1985) equation was altered so that the curve intercepts the hourly ingestion rate given by Båmstedt and Karlson (1998) at the copepod concentrations that they used; hence, the hourly ingestion rate becomes

$$\log_{10}G = 0.746\log_{10}C + 1.092. \quad (5)$$

Ingestion rate was converted to joules assuming that 1000 µg DW copepod material = 26 J (Omori and Ikeda 1984).

Ingestion rate: phytoplankton

Phytoplankton supplements the mainly carnivorous diet of northern krill (e.g. McClatchie 1985; Båmstedt and Karlson 1998). Nevertheless, the amount of chlorophyll pigment in the guts becomes relatively high when krill enter phytoplankton-rich layers (see Mauchline 1960). In the Clyde Sea in July 1996, for instance, chlorophyll *a* (Chl *a*) was relatively high at 16.15 mg·L^{-1} between 20 and 10 m (Table 2). Krill showed a diel cycle in the Chl *a* pigment content in their guts, peaking during the night at around 4 µg Chl *a*·individual^{-1} and dropping to virtually nothing during the day (P. Mayzaud, unpublished data). Given a gut transit time of 60 min (P. Mayzaud, unpublished data), this gives a total daily intake of 20 µg Chl *a*·individual^{-1}, equivalent to 23.5 J of energy assimilated (assuming an assimilation efficiency (S) of 0.8; Lasker 1966). This is approximately half of the daily energy requirement that we have calculated for an average-sized adult krill in the Clyde during summer (43 J for a 93 mg DW krill at 9°C).

At concentrations at or above 16.15 mg Chl *a*·L^{-1}, phytoplankton feeding is assumed to meet half the daily metabolic requirement of the individual such that net energy gain per hour becomes

$$H_{ij} = \frac{(G_{ij}S) - (1 - P_{ij})M_{ij}}{1 - P_{ij}} \quad (6)$$

where

Table 2. Average Chl *a* concentration and copepod biomass at midday and midnight in defined depth intervals in the Clyde Sea and the Kattegat.

Clyde Sea depth interval (m)	Chl *a* ($mg \cdot L^{-1}$)	Daytime biomass ($\mu g \cdot L^{-1}$)	Nightime biomass ($\mu g \cdot L^{-1}$)	Kattegat depth interval (m)	Daytime biomass ($\mu g \cdot L^{-1}$)	Nightime biomass ($\mu g \cdot L^{-1}$)
10–0	16.12	3.10	14.20	20–0	12.54	21.91
20–10	16.15	2.64	32.94	40–20	15.72	3.05
40–20	10.71	8.09	5.04	60–40	12.42	11.70
60–40	4.78	5.17	0.24	80–60	7.12	9.85
80–60	1.85	1.27	0.37	100–80	15.13	9.76
100–80	0.80	0.24	0.32	115–100	14.42	15.55
120–100	0.95	0.06	0.19			
135–120	1.10	0.12	0.35			

$$(7) \qquad P_{ij} = 0.5\left[\frac{\text{Chl } a}{16.15}\right]$$

and Chl *a* is equal to the concentration of phytoplankton (milligrams per litre). This means that where the concentration of Chl *a* is below the maximum level, i.e., 16.15 $mg \cdot L^{-1}$, the relative hourly contribution from phytoplankton feeding to the total energy intake becomes reduced in a linear fashion.

Parameters for calculating expected probability of mortality (*E*)

Visual predation

Visual fish predators were assumed to be the principal source of mortality of krill in the upper layer water column of the Clyde Sea and the Kattegat (Tanasichuck 1999). The expectation that a krill will encounter a fish in the upper layers (*e*) is calculated as a function of visual range (*r*), speed (*v*), and density of the predator (*N*) and the size of the prey (following Eggers 1977):

$$(8) \qquad e = \theta \pi r^2 v N \mathrm{d}t$$

where θ is the field of view of the fish and d*t* is the time interval (other units as in Table 1).

It is assumed that each encounter (*e*) results in death of the krill prey, so the expectation of mortality (*E*) of an individual krill may be calculated as

$$(9) \qquad E = 1 - \exp(-e\mathrm{d}t).$$

The parameter *E* is a probability function so that, if scaled up to the population level, the value would represent the proportion of individuals lost to the population per unit time as a result of visual predation. Predator visual range *r* is obtained from an equation developed by Aksnes and Giske (1993) and may be calculated through a Newton–Raphson iteration:

$$(10) \qquad r^2 \exp(c_z r + zK) = \rho I_s \left| C_0 \right| A_{zp} \Delta S_e^{-1}$$

where *z* is depth, c_z is the local beam attenuation coefficient, *K* is the local diffuse attenuation coefficient, ρ is the light fraction lost at the surface (0.5; Aksnes and Giske 1993), I_s is the irradiance at the surface, C_0 is the inherent contrast of krill (0.5; Aksnes and Giske 1993), A_{zp} is the krill cross-sectional area, and ΔS_e is the sensitivity of the eye of the planktivore (3.0×10^{-6} $\mu mol \cdot m^{-2} \cdot s^{-1}$; Rosland and Giske 1994). Values for the parameters are given in Table 1.

Tactile predation

In the deeper layers where visual predation levels are extremely low, it is believed that that bottom-dwelling tactile fish predators such as cod add marginally to the level of *E*, given the high levels of northern krill found in cod stomachs (F. Buchholz, unpublished data). This factor was built in through increasing the calculated level of visual predation by two orders of magnitude in the deepest layer and by one order of magnitude in the next layer up. Furthermore, the level of visual predation in these layers was not allowed to decrease below the level observed at 12:00.

Production requirements of krill

According to Lasker (1966), the percentage investments from assimilated energy for *Euphausia pacifica* were as follows: respiration, 67%; growth, 9%; reproduction, 9%; moulting, 15%. If the respiration rate of the krill is known, then the energy demand for growth, reproduction, and moulting can be inferred. In eq. 3, respiration was a function of temperature and body size. Given that temperature varies with depth, total energy respired over a 24-h period will depend on the exact vertical migration behaviour. The vertical migration profile is nevertheless an output of the model, while growth, reproduction, and moulting represent energy targets to be fixed at initial parameterisation. To use the relationship provided by Lasker (1966) in order to estimate the amount of energy required for growth, reproduction, and moulting, therefore, it was necessary to infer an average temperature occupied by krill over a 24-h period. In both the Clyde Sea and the Kattegat, field data indicated that the average depth occupied when considering the mean of the daytime and nighttime distributions was approximately 70 m. At this depth, the temperature was 9.2°C in the Clyde Sea and 6.2°C in the Kattegat. Body size was set at the modal size-class of the adult population, which was 39 mm (93 mg DW) in the Clyde Sea and 34 mm (6.154 mg DW) in the Kattegat (G.A. Tarling, unpublished data). The resulting value for the hourly respiration rate, provided by eq. 3, was converted to daily respiration rate through multiplication by 24. Daily rates for growth, reproduction, and moulting were then calculated as proportions of daily respriration rate following the values given by Lasker (1966) and presented in Table 3.

Environmental data sets

Energy gain (H)

Data used to calculate the energy budget are principally taken from sampling missions carried out during July and August 1996 in the Clyde Sea and the Kattegat onboard R/V *Heincke*. Depth-discrete estimates of Chl *a* profiles and copepod biomass are presented in Table 2 and are described further in Lass (1998). The copepod data in Table 2 were obtained from midnight and midday net deployments, and these were assumed to be representative of daytime and nighttime situations. To simulate the transition period between these two situations, a sliding mean function was applied to the dusk (20:00–22:00) and dawn (04:00–06:00) periods. Temperature profiles are presented in Fig. 1.

Table 3. Daily rates of energy demand for growth, reproduction, and moulting as proportions of respiration rate in the Clyde Sea and the Kattegat following the proportional values given in Lasker (1966).

	Respiration ($J \cdot day^{-1}$)	Growth ($J \cdot day^{-1}$)	Reproduction ($J \cdot day^{-1}$)	Moulting ($J \cdot day^{-1}$)	Total energy demand ($J \cdot day^{-1}$)
Clyde Sea	28.6	3.8	3.8	6.4	42.7
Kattegat	14.3	1.9	1.9	3.2	21.3

Fig. 1. Typical temperature profile of (*a*) the Clyde Sea and (*b*) the Kattegat during summer environmental conditions (April–May and July 1996).

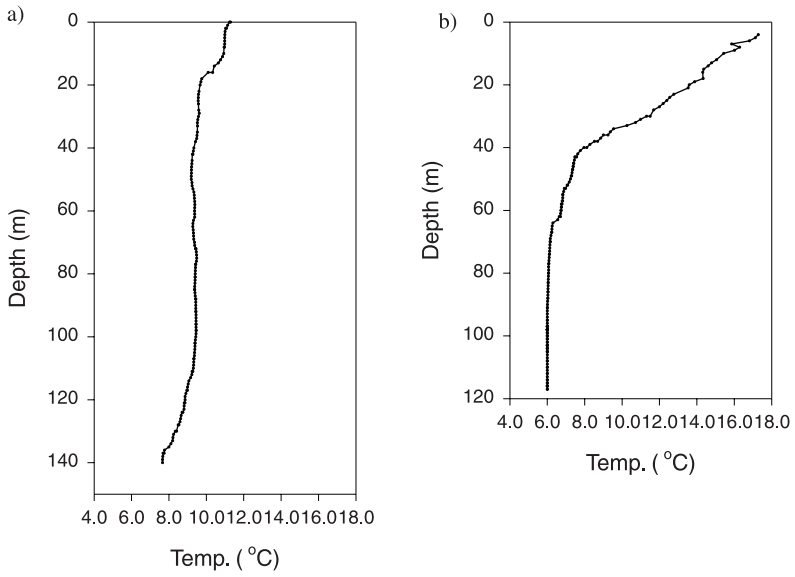

Fig. 2. Light intensity profile used in the Clyde Sea and Kattegat models taken from a typical day during the PEP programme summer sampling mission.

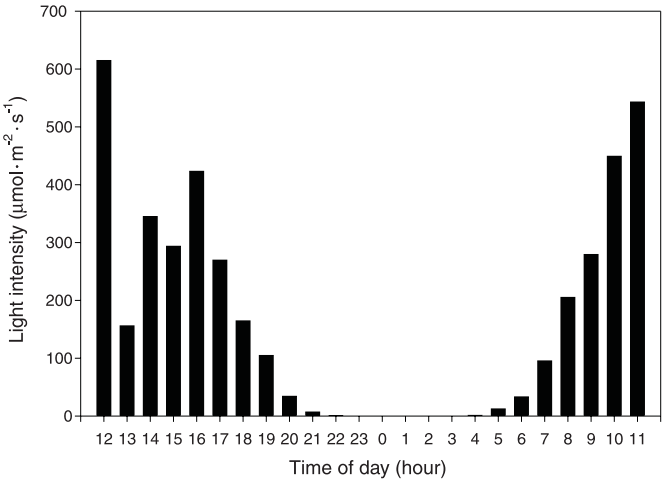

Expectation of mortality (E)

Levels of irradiance were taken from a typical 24-h period during the Clyde Sea and Kattegat sampling missions using data from the irradiance meter onboard R/V *Heincke* (Fig. 2) (note that absolute values were found to be offset, so both data sets were reset to a peak value of 98 μeinsteins$\cdot m^{-2} \cdot s^{-1}$). The attenuation coefficient (K) was measured at 0.2881 in the Clyde Sea and 0.1213 in the Kattegat using a diffuse-light transmissometer. The c_z is assumed to be three times K. A value of $0.01 \cdot m^{-3}$ was taken as the fish density in the Clyde Sea and $0.001 \cdot m^{-3}$ as that in the Kattegat. The implications of setting these fish density values are explored in the sensitivity analyses.

Parameter matrices

The parameter matrices $\{H_{ij}\}$ and $\{E_{ij}\}$ for the Clyde Sea consisted of eight depth intervals (j) covering a 135-m water column. For the Kattegat, there were six depth intervals (j) covering a 115-m water column. The total time period was 24 h in both environments, divided into hourly intervals (i). The net energy balance (H) for each cell (ij) was calculated as follows according to eq. 6.

Model run procedure

At the start of the model run, a net energy gain target for the 24-h period (H_t) is set such that it is equal to the daily requirement to grow (g), reproduce (s), and moult (w) such that

$$H_t = g + s + w \quad (11)$$

(see Table 3 for values of g, s, and w). An iteration procedure (Microsoft Excel 97 Solver: Generalized Reduced Gradient (GRG2) nonlinear optimization) is run until the optimal solution to the following problem is found under the constraint that the krill must spend and cannot exceed 1 h in each of the 24 time intervals (i) such that

$$\sum_{i=1}^{i=24} H_{ij} > H_t \text{ and } \sum_{i=1}^{i=24} E_{ij} = \min E. \quad (12)$$

For the Clyde Sea, H_t was set at 14 $J \cdot day^{-1}$, while for the Kattegat, it was 7 $J \cdot day^{-1}$ (see Table 3).

No constraint is placed on the animal with respect to moving from one depth interval to any other between time intervals.

Tarling et al. (1998*a*) observed upward swimming speeds above 7 $cm \cdot s^{-1}$ and downward swimming speeds as high as 11 $cm \cdot s^{-1}$ in northern krill in the Mediterranean Sea. This would equate to a total distance travelled of 252 m upwards and 396 m downwards per hour. These distances are twice as great as the depth of the water column at either of the study sites and illustrate that this animal is capable of rapid movement between any of the depth intervals defined in this model. A further assumption is that there is no additional metabolic cost in moving between depth intervals. This assumption is based on the work of Kils (1981), who showed that Antarctic krill (*Euphausia superba*) are capable of swimming at speeds of up to 15 $cm \cdot s^{-1}$ without affecting their standard metabolism. This is because krill regulate their speed mainly by changes in the execution of the pleopod swimming stroke. At 15 $cm \cdot s^{-1}$, the stroke is maximally executed. Above 15 $cm \cdot s^{-1}$, stroke frequency must be increased, which then raises metabolic rate to an "active metabolism." Northern krill, although smaller, have the same basic design as Antarctic krill, and it is believed that the reduction in propulsive force from the comparatively smaller pleopods is counteracted by a corresponding decrease in the resistance of the body moving through the water, since both parameters are a function of the surface area. To achieve upward rather than horizontal swimming, krill must change their body angle so that most of the propulsive force is projected into the vertical rather than the horizontal vector, in much the same way as an aerofoil (Kils 1981). A rise in standard metabolism is therefore not expected at the rate of movement between depth intervals predicted by the model, and so only standard metabolic rates are used in model parameterisations.

Results

Parameter matrices

The energy budget matrix calculated for the Clyde Sea is presented in Fig. 3*a* and for the Kattegat in Fig. 3*b*. For the Clyde Sea, depth intervals below 60 m have a negative energy balance at any time of day as a result of the low food availability and hence low energy intake that cannot compensate for the cost of respiration. Above this depth, the energy balance is mostly positive, although there is variation according to time of day as the copepod biomass migrates out of one depth interval and into another.

For the Kattegat, the energy balance is almost wholly positive at any depth, with the deepest depth interval being the most profitable in terms of energy gain. Furthermore, this depth layer does not oscillate in terms of energy balance over the 24-h period, since the relatively high copepod biomass remains at a steady level. Closer to the surface, it is apparent that some layers are more profitable during daytime and that other layers are more profitable at night as the copepod community performs DVM. The 40- to 20-m layer, for instance, switches from being a relatively high-profit depth interval during daytime to a slightly negative environment at night, while the reverse occurs between 20 m and the surface.

Values for each cell (*ij*) in the expectation of mortality matrix were obtained from the calculation of eqs. 10, 8, and then 7. The resulting matrix for the Clyde Sea is shown in Fig. 3*c* and for the Kattegat in Fig. 3*d*. In the Clyde Sea during daytime, it is apparent that depth intervals above 20 m have values for E that are many orders of magnitude greater than those below 20 m. During night, this difference drops to within three orders of magnitude. It should also be noted that although the deepest depth intervals have been altered to include the effect of bottom-feeding fish, visual predation remains the dominant influence on the general shape of the expectation of mortality matrix. The expectation of mortality matrix in the Kattegat has the same general shape as in the Clyde Sea, although the lower K in the Kattegat makes values of E comparatively higher at deeper depth intervals.

Optimal time allocations

The optimal time allocation within the depth–time matrix under the given constraints for the Clyde Sea is presented in Fig. 4*a*. It is apparent that the krill have a daytime depth of between 60 and 40 m during most of the daytime period. At 22:00, they begin an upward migration into the 40- to 20-m depth interval and then enter the 20- to 10-m layer after 01:00 where they remain until 04:00. By 06:00, the krill have returned to their daytime depth between 60 and 40 m.

In Fig. 5*a*, the rate at which energy is gained (H_t' per hour) is compared with the expected rate of mortality E (per hour). For most of the daytime period, H_t' is close to zero or even slightly negative. The principal period of H_t' is during nighttime, which corresponds to the period when the krill occupy depth intervals that are closer to the surface. Between 01:00 and 04:00, H_t' values are up to 6 $J \cdot h^{-1}$. Correspondingly, this period is also the time when the krill experience their E, rising from a daytime level of close to zero to 0.000269$\cdot h^{-1}$. The net H_t' from this optimal time allocation strategy was equal to the target H_t (14 $J \cdot day^{-1}$). The E was 0.000994$\cdot day^{-1}$. Details on the division between copepod and phytoplankton ingestion and the cost of respiration are presented in Table 4.

The optimal time allocation strategy for the Kattegat under the given constraints is presented in Fig. 6*a*. Krill occupied the 100- to 80-m depth interval for the midday period (11:00–16:00) but otherwise spent the majority of their time between 80 and 60 m. The only other movement predicted was into the 60- to 40-m depth interval between 04:00 and 05:00. In Fig. 5*b*, it is apparent that H_t' was relatively steady and positive over the entire 24-h period. The highest rates of around 1.5 $J \cdot h^{-1}$ corresponded to the occupation of the 100- to 80-m depth interval between 11:00 and 16:00 and also the brief movement into the 60- to 40-m depth interval at 04:00. The lowest rates of 0.5 $J \cdot h^{-1}$ corresponded to the time spent in the 80- to 60-m depth interval. Values for E showed a marked difference between day and night, with values as high as 0.0012$\cdot h^{-1}$ being experienced between 11:00 and 16:00, while nighttime values were close to zero.

The net H_t' from this optimal time allocation strategy was higher (19.42 $J \cdot day^{-1}$) than the target H_t (7 $J \cdot day^{-1}$). The E was 0.009082$\cdot day^{-1}$. Details on the division between copepod and phytoplankton ingestion and the cost of respiration are presented in Table 4.

Sensitivity analyses

Predation levels

The density of predators in the original runs of the model were assigned as 0.01$\cdot m^{-3}$ in the Clyde Sea and 0.001$\cdot m^{-3}$ in the Kattegat, since these densities produced values for E within an order of magnitude of the mortality rate of 0.0003$\cdot day^{-1}$ (i.e., the proportion lost to the population each day) that was predicted for northern krill by Labat and

Fig. 3. Depth–time matrices (covering the entire water column over a 24-h period) of the net energy gain in (*a*) the Clyde Sea and (*b*) the Kattegat and the expected mortality rate (as a proportion of the population) in (*c*) the Clyde Sea and (*d*) the Kattegat. Each matrix cell covers a depth interval of between 10 and 20 m and a time period of 1 h.

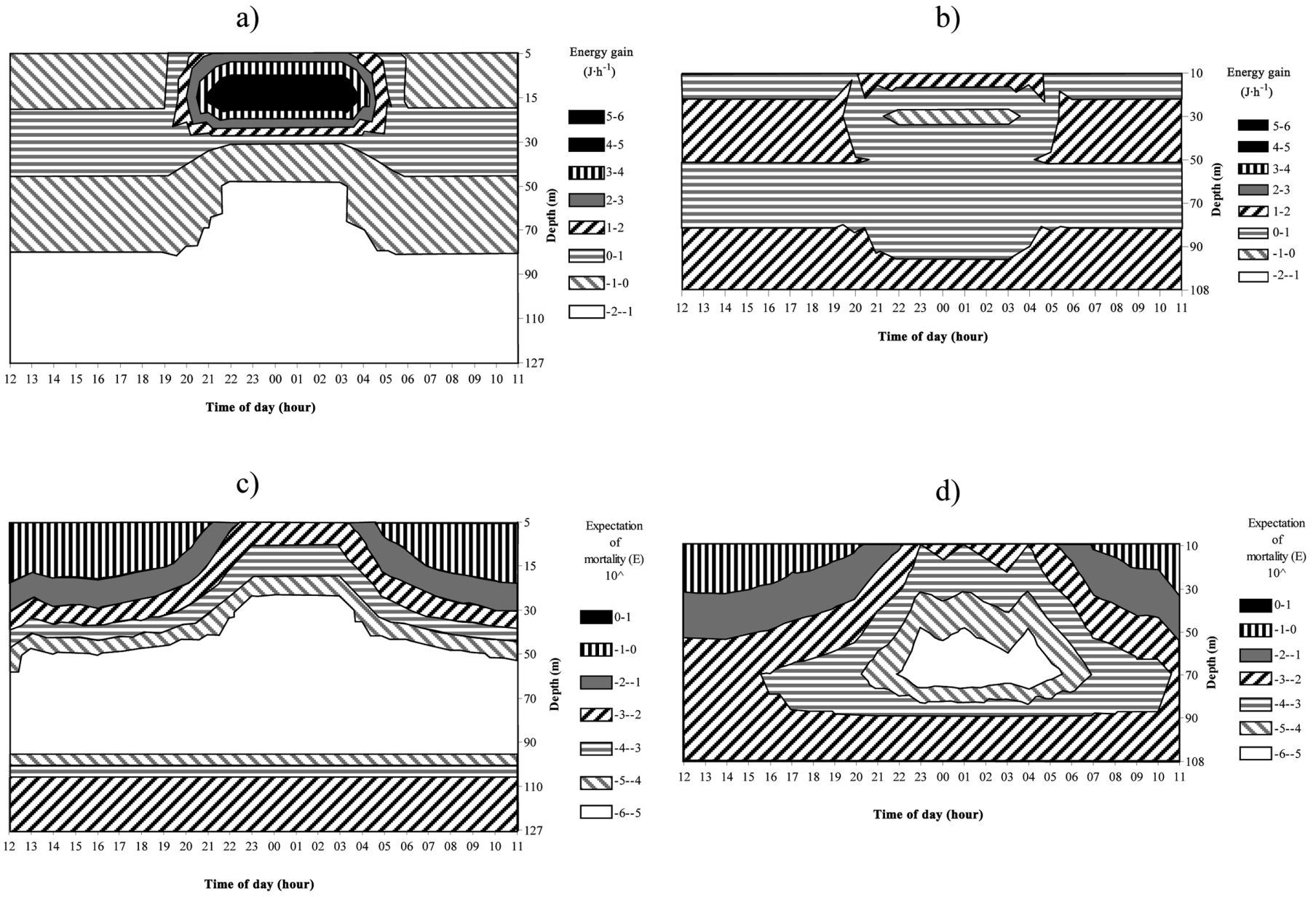

Fig. 4. Optimal time allocation strategy for a krill in the Clyde Sea (*a*) allowed to feed continuously over a 24-h period (fish density = $0.01 \cdot m^{-3}$), (*b*) when fish density is $0.0001 \cdot m^{-3}$ (continuous feeding over 24 h), and (*c*) constrained from feeding during the daytime (fish density = $0.01 \cdot m^{-3}$) (time allocation: horizontally hatched bars, >0 to 30 min; diagonally hatched bars, 30 min to <1 h; solid bars, 1 h). (*d*) Net-catch concentrations (MOCNESS, 1 m^2) of northern krill in the Clyde Sea between 4 and 5 July 1996 (local time of catch indicated at the top of each graph).

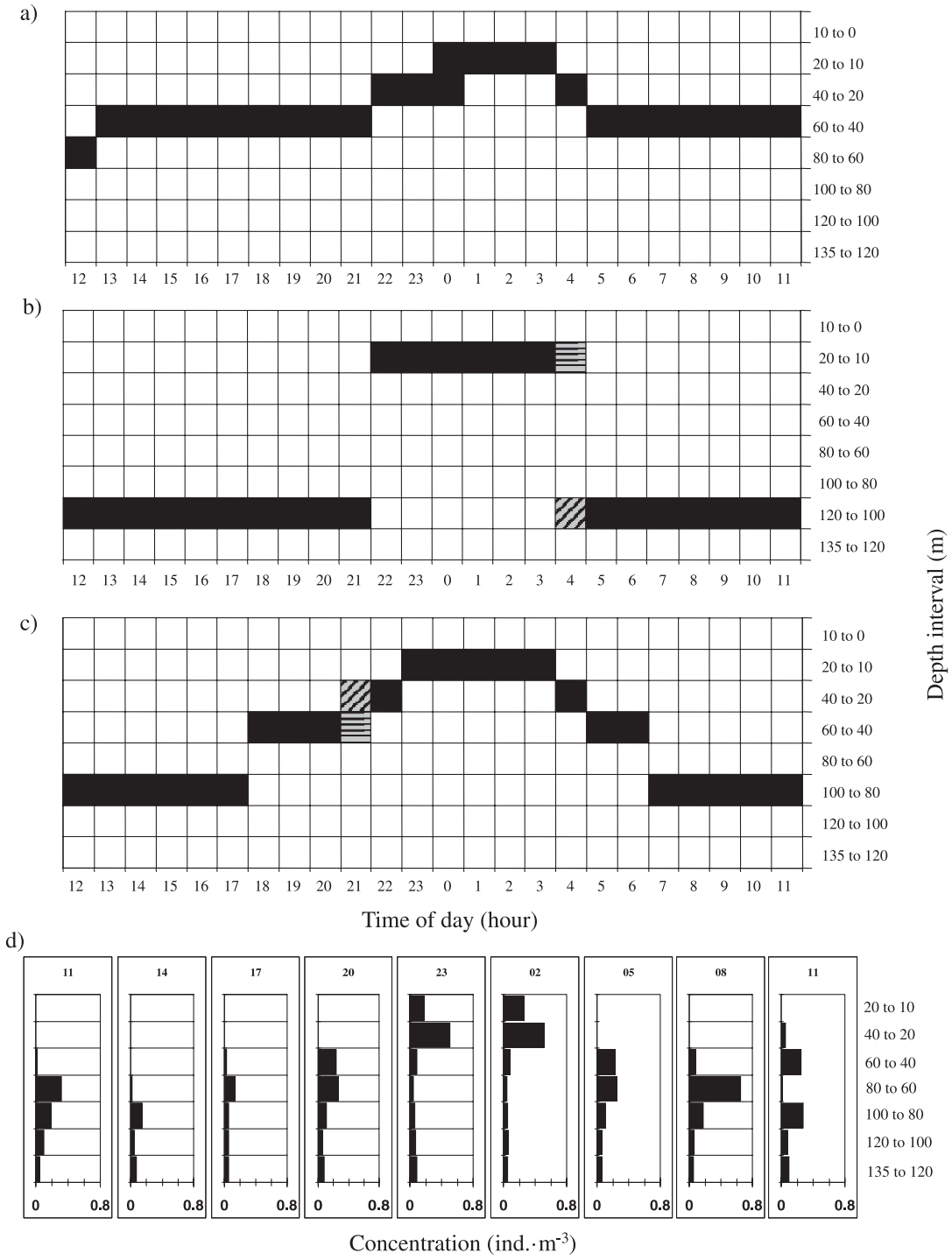

Cuzin-Roudy (1996) in the Ligurian Sea. The model was run with the density of predators increased and decreased by two orders of magnitude to investigate the effect of varying predator numbers on model predictions. When predator density was increased, the time allocation strategy remained the same in both the Clyde Sea and the Kattegat, although E increased to $0.10 \cdot day^{-1}$ in the Clyde Sea and to $0.89 \cdot day^{-1}$ in the Kattegat. This showed that when predator densities rise above 0.01 individual$\cdot m^{-3}$ in the Clyde Sea and 0.01 individual$\cdot m^{-3}$ in the Kattegat, the relative difference in risk between depth intervals remains approximately the same. Therefore, the model predicts that vertical migration behaviour does not

Fig. 5. Optimal time allocation strategy for a krill over a 24-h period in the Kattegat (*a*) allowed to feed continuously (fish density = $0.001 \cdot m^{-3}$), (*b*) when fish density is $0.00001 \cdot m^{-3}$ (continuous feeding for 24 h), (*c*) constrained from feeding during the daytime (fish density = $0.001 \cdot m^{-3}$) (time allocation: horizontally hatched bars, >0 to 30 min; diagonally hatched bars, 30 min to <1 h; solid bars, 1 h). (*d*) Net-catch concentrations (MOCNESS, 1 m^2) of northern krill in the Kattegat between 18 and 19 July 1996 (local time of catch indicated at the top of each graph).

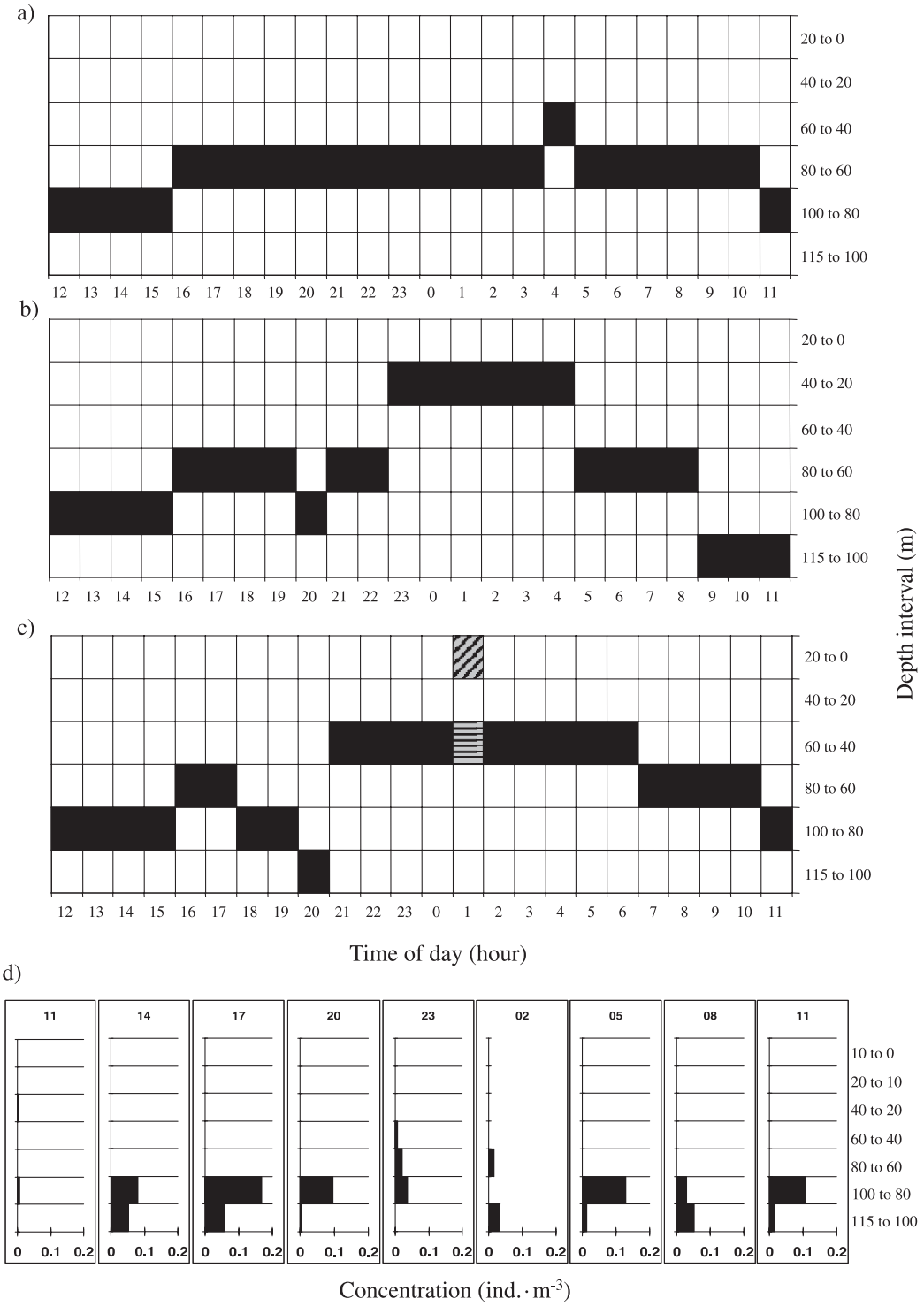

change when there is a large influx of visual predators. When the predator density was decreased, the time allocation strategy did change such that the krill increased their time spent in the low risk, low energy gain environments and also in the high risk, high energy gain environments. For the Clyde Sea, this meant residence in the lowermost (low energy gain) depth intervals during daytime and the uppermost (high energy gain) depth intervals during night

Table 4. Contribution to net energy gained (H_t') from copepod and phytoplankton ingestion, the loss to respiration, and the expected mortality rate (E) as a proportion of the population resulting from following the optimal time allocation strategy in the Clyde Sea and the Kattegat where feeding was continuous over 24 h and where feeding was constrained during daytime (fish density = $0.01 \cdot m^{-3}$ in the Clyde Sea and $0.001 \cdot m^{-3}$ in the Kattegat).

	H_t' ($J \cdot day^{-1}$)	E	Energy from copepods ($J \cdot day^{-1}$)	% of total body energy	Energy from phytoplankton ($J \cdot day^{-1}$)	% of total body energy	Energy for respiration ($J \cdot day^{-1}$)	% of total body energy
Continuous feeding								
Clyde Sea	14.000	0.000994	27.841	1.273	15.134	0.692	28.975	1.325
Kattegat	19.416	0.009082	33.641	1.539	0.076	0.003	14.301	0.654
Constrained feeding								
Clyde Sea	14.000	0.001492	23.890	1.093	19.329	0.884	29.219	1.336
Kattegat	7.050	0.013175	21.983	1.005	0.106	0.005	15.039	0.688

(Fig. 4*b*). For the Kattegat, low-gain environments occur in the midpart of the water column, while high gain occurs in both the deep and surface layers. Therefore, the pattern here was movement from midwater to the surface around midnight and from midwater to deep around midmorning (Fig. 6*b*).

Overall, the model predicts that when fish density is high, the optimal strategy is to maximise time in medium risk, medium energy return environments. In low fish density situations, greater time may be spent in the higher risk environments where most of the day's energy requirements may be obtained, thus allowing the krill to spend the majority of the day in very low risk, low energy return environments.

Temperature

The effect of temperature stratification was investigated by making the water column a uniform temperature. Two runs were carried out, one using the maximum temperature observed and the other using the minimum temperature. There was very little difference in the resulting time allocation strategies for either temperature that was used in both the Clyde Sea and the Kattegat. Temperature was therefore not considered particularly important in influencing predicted migration patterns.

Krill feeding strategy

The model assumed that krill were able to feed continuously over the 24-h period. A further constraint was added so that krill could only feed during "nighttime" (18:00–06:00). In both the Clyde Sea and the Kattegat, the resulting time allocation strategies produced higher values for E than for the original model runs (Table 4). This is to be predicted, since the krill must increase time in the higher energy gain, higher risk environments, as there is a shorter time available in which to feed. In the Clyde Sea, the krill move above 40 m by 22:00 and then occupy the 20- to 10-m depth interval for 5 h. During daytime, when the model constrains the krill from feeding, their optimal strategy is to occupy the lowest risk environment between 100 and 80 m (Fig. 4*c*). For the Kattegat, the optimal strategy is to occupy the 60- to 40-m depth layer during the period when the model allows krill feeding and then to spend an hour in the high risk, high energy gain environment at the surface and an hour in the deepest depth interval. Periods when feeding is not allowed are spent between 60 and 100 m (Fig. 6*c*).

Discussion

A MOCNESS net was used over a 30-h period in the Clyde Sea and the Kattegat to investigate the vertical migration behaviour of northern krill (see Tarling et al. 1998*b*). The results of the net-catch study are presented in Figs. 4*d* and 6*d*. For the Clyde Sea, the original run of the model predicted a daytime distribution that was between 20 and 40 m higher than found in the field observations. Nevertheless, both the predicted timing of the nighttime migration into and out of the upper layers and the upper depth limit of migration closely matched observations. The predictions of the model run with the added constraint on feeding during daytime were closer to the observed daytime depth of the krill population. The predicted timing of upward migration and the upper migration limit were also similar to observations. For the Kattegat, there was little predicted vertical movement during nighttime in the original run of the model, unlike that inferred from the net-catch data (see Tarling et al. 1998*b*). However, the predicted daytime depth of below 80 m was similar to observations. As with the Clyde Sea, the constraint on feeding during daytime produced model predictions that were closer to field observations. In this instance, upward migration during nighttime was predicted, although the predicted daytime depth was occasionally one depth interval higher than observed.

The comparison of model predictions in the Clyde Sea and the Kattegat illustrates that the model is successful in predicting DVM in two localities with contrasting distributions of food and predation risk. The model would therefore seem to be a good representation of the true processes controlling the vertical migration behaviour of northern krill. This assumes that krill in the Clyde Sea and the Kattegat have a common response to patterns of light levels (determining vulnerability to predators) and distributions of food. Furthermore, the sensitivity of model predictions to variations in predator density and feeding regime show that it is food and predation risk that drive the predicted DVM patterns. The lack of sensitivity to temperature effects on metabolic costs shows that the model predicts this to be a relatively minor influence on DVM patterns.

Feeding

Field observations of northern krill show a clear pattern of DVM in both the Clyde Sea and the Kattegat. The Clyde Sea has relatively weak thermal stratification and high concentra-

Fig. 6. Rate of energy gain and expected mortality for a krill following the optimal time allocation strategy over a 24-h period in (*a*) the Clyde Sea when allowed to feed continuously (fish density = $0.01 \cdot m^{-3}$), (*b*) the Kattegat when allowed to feed continuously (fish density = $0.001 \cdot m^{-3}$), and (*c*) the Kattegat when constrained from feeding during the daytime (fish density = $0.001 \cdot m^{-3}$).

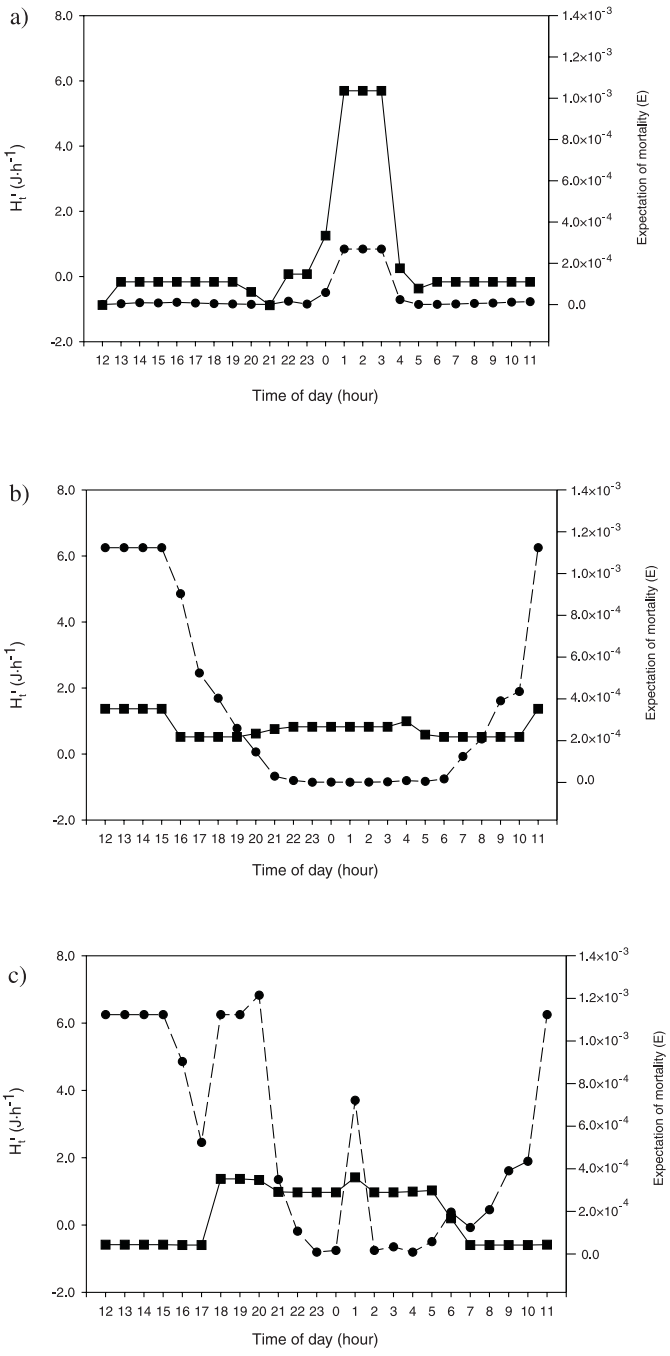

tions of food items (both phytoplankton and copepods) in the surface layers, and consequently relatively high light attenuation near the surface. This contrasts with deep trench habitats in the Kattegat, where there is a strong thermocline (10°C gradient) and a relatively even distribution of food items (principally copepods) through the water column, with less attenuation near the surface. As a result of these differences, the model predicts more pronounced DVM in the Clyde Sea than in the Kattegat. At greater depths in the Clyde Sea, food is comparatively less abundant than in the Kattegat, yet because of the greater light attenuation, predation risk is also reduced relative to the Kattegat. To achieve the same level of food intake as in the Kattegat, the krill in the Clyde Sea must ascend to nearer the surface at night. Likewise, the krill in the Kattegat must go deeper by day to minimise predation risk. Because prey is distributed throughout the water column in the Kattegat, these animals need not ascend so much as in the Clyde Sea. The model successfully reproduces these intersite differences in DVM as a direct result of the difference in prey and light attenuation.

One interesting further feature was that model predictions for DVM were closer to field observations in both the Clyde Sea and the Kattegat when a constraint of feeding during the daytime was imposed. The ability of the krill in the Kattegat to feed on a rich community of copepods during the daytime results in a model predicting only a weak vertical migration into the upper layers at night. However, with the added feeding constraint, a more pronounced migration is predicted, closer to the patterns observed in the field. The laboratory experiments of Båmstedt and Karlson (1998) indicated that northern krill showed no diel rhythm in feeding activity, and field data from Onsrud and Kaartvedt (1998) indicated that northern krill fed on copepods day and night. This is in contrast with the results of the PEP programme (Lass 1998; J. Matthews, unpublished data) where it was found that the stomach contents of northern krill in the deep layers of the Kattegat during daytime primarily contained a copepod species (*Temora longicornis*) that was exclusively found in the surface layers. This suggests that the majority of feeding activity occurred during the nighttime period when the krill moved into the upper layers. The fact that model predictions were closer to observed patterns when krill were constrained from feeding during daytime supports the hypothesis that krill may exhibit a diel rhythm in feeding activity in certain environments. What is also evident from the model is that undertaking a diel feeding rhythm also results in a greater expectation of mortality, as the animal enters riskier environments to obtain a greater feeding rate in the limited time available. Therefore, undertaking a diel feeding rhythm may indicate that there are extra costs in feeding in the deeper layers during daytime that have not been considered here. For instance, feeding makes the foraging zooplankton less transparent (see Giske et al. 1994), which may present greater risks in the dim light levels in the deep during daytime than at the surface during the night. Also, the deeper layers contained a greater proportion of *Calanus* (Lass 1998; J. Matthews, unpulished data), which are larger and are more likely to have a stronger escape response than the smaller *Temora* at the surface.

Predation levels

Unlike the Clyde Sea, where predation risk is highest during the nighttime, in the Kattegat, predation risk is highest during the day, even when the feeding constraint is added. This highlights the fact that the Kattegat is a riskier environment than the Clyde Sea for two reasons. Firstly, the attenu-

ation coefficient is lower, resulting in greater light penetration and greater risk of visual predation at the middle of the water column. Secondly, the water column is shallower, so a movement to depth to avoid visual predation results in the animals being near bottom and close to tactile bottom-dwelling predators. Therefore, whereas the Clyde Sea krill may take refuge during the daytime from predation in the middle of the water column where there is little visual or tactile predation, krill in the Kattegat must trade-off the relative risk of one predation type with another. During the daytime, the risk from bottom-dwelling predators is much less than that from visual predators and a deep daytime distribution is preferable.

Mortality rates for zooplankton are inherently difficult to estimate (McGurk 1986), and although the presence or absence of major predators may be indicated by pelagic trawls and multifrequency acoustics (Kaartvedt et al. 1996), gaining estimates of fish predator density is beyond the scope of current oceanographic study. Sensitivity analyses were used to predict the effect of altering fish densities over two orders of magnitude on the DVM pattern. Although estimating predation levels is a weakness in trade-off models, the present model design places much greater reliance on estimating the relative rather than the absolute risk of predation throughout the water column. In this sense, therefore, the accuracy of the model predictions depend much more on the foraging ability of the fish predator under light levels that change according to depth and time of day, which are aspects that have been modelled and validated to an accurate degree (Fiksen et al. 1998 and references therein). The biggest improvement to the predation aspect of the model will be in determining the risk from less visually dependent bottom-dwelling predators such as cod in relation to their visual pelagic counterparts.

What has been presented is a framework that is able to simulate migration patterns based on a set of forcing functions either obtained from the literature or measured directly from field sampling campaigns. Further data sets will no doubt improve the functions that are used so that real values for parameters are represented more accurately in simulations. It is also necessary that certain important assumptions in this approach, such as the freedom of movement between any depth interval and the lack of any added metabolic costs to vertical migration, be examined in greater detail. However, the power of this approach is in allowing the modeller to compare and contrast different DVM strategies where only relative vertical profiles of mortality risk and metabolic gain are reliable.

Acknowledgements

We would like to thank the following people for their assistance in field sampling and workshops that took place as part of the PEP programme: E. Albessard, S. Bröhl, C. Buchholz, J. Cuzin-Roudy, S. Dallot, P. David, K. Grau, O. Guerin, M. Hatherell, J.-P. Labat, S. Lass, D. Müller-Navarra, P. Schumann, S. Sabini, M. Salomon. and P. Virtue. We would also like to acknowledge the support and efficiency of the crew of R/V *Heincke*. This project was funded by EU-MAST III (Marine Science and Technology programme), Physiological Ecology of a Pelagic Crustacean (PEP) project (MAS3-CT-0013). G.A.T. was supported by an NERC MSTB targeted fellowship entitled "Advective ecology of zooplankton in the Clyde Sea" (GST/59818MS).

References

Aksnes, D.L., and Giske, J. 1993. A theoretical model of aquatic visual feeding. Ecol. Model. **67**: 233–250.

Angel, M.V. 1985. Vertical migrations in the oceanic realm, possible causes and probable effects. *In* Migration mechanisms and adaptive significance: contributions in marine science. *Edited by* M.A. Rankin. Marine Science Institute, University of Texas at Austin, Port Aransas, Tex. pp. 45–70.

Båmstedt, U., and Karlson, K. 1998. Euphausiid predation on copepods in coastal water of the Northeast Atlantic. Mar. Ecol. Prog. Ser. **172**: 149–168.

Bollens, S.M., and Frost, B.W. 1989. Zooplanktivorous fish and variable diel vertical migration in the marine plankton copepod *Calanus pacificus*. Limnol. Oceanogr. **34**: 1072–1083.

Buchholz, F., David, P., Matthews, J.B.L., Mayzaud, P., and Patarnello, T. 1998. Impact of a climatic gradient on the *P*hysiological *E*cology of a *P*elagic crustacean (PEP). Proc. 3rd Eur. Mar. Sci. Technol. Conf. Vol. I. Marine systems. Office for Official Publications of the European Communities, Luxembourg. pp. 39–48.

Eggers, D.M. 1977. Plankivore preference by prey size. Ecology, **77**: 46–59.

Fiksen, O., Utne, A.C.W., Aksnes, D.L., Eiane, K., Helvik, J.V., and Sundby, S. 1998. Modelling the effect of light, turbulence and ontogeny on ingestion rates of larval cod and herring. Fish. Oceanogr. **7**: 355–363.

Gilliam, J.F., and Fraser, D.F. 1987. Habitat selection under predation hazard: test of a model with foraging minnows. Ecology, **68**: 1856–1862.

Giske, J., Aksnes, D.L., and Fisken, O. 1994. Visual predators, environmental variables and zooplankton mortality risk. Vie Milieu, **44**: 1–9.

Huntley, M., and Brooks, E.R. 1982. Effects of age and food availability on diel vertical migration of *Calanus pacificus*. Mar. Biol. **71**: 23–31.

Ikeda, T. 1985. Metabolic rates of epipelagic marine zooplankton as a function of body mass and temperature. Mar. Biol. **85**: 1–11.

Ikeda, T., and Motoda, S. 1978. Estimated zooplankton production and their ammonia excretion in the Kuroshio and adjacent seas. Fish. Bull. U.S. **76**: 357–367.

Johnson, G.H., and Jakobsen, P.J. 1987. The effect of food limitation on vertical migration in *Daphnia longispina*. Limnol. Oceanogr. **32**: 23–31.

Kaartvedt, S., Melle, W., Knutsen, T., and Skjoldal, H.R. 1996. Vertical distribution of fish and krill beneath water of varying optical porperties. Mar. Ecol. Prog. Ser. **136**: 51–58.

Kils, U. 1981. Swimming behaviour, swimming performance and energy balance of Antarctic krill, *Euphausia superba*. BIOMASS Sci. Ser. No. 3.

Krebs, J.R., and Davies, N.B. 1991. Behavioural ecology: an evolutionary approach. Blackwell Scientific Publications, Oxford, U.K.

Labat, J.P., and Cuzin-Roudy, J. 1996. Population dynamics of the krill *Meganyctiphanes norvegica* (Sars) (Crustacea: Euphausiacea) in the Ligurian Sea (N-W Mediterranean Sea). Size structure, growth and mortality modelling. J. Plankton Res. **18**: 2295–2312.

Lasker, R. 1966. Feeding, growth, respiration and carbon utilization of a euphausiid crustacean. J. Fish. Res. Board Can. **23**: 1291–1317.

Lass, S. 1998. Untersuchungen zur Nahrungsökologie von *Meganyctiphanes norvegica*. Diploma thesis, Christian Albrechts Univerität, Kiel.

Longhurst, A.R. 1976. Vertical migration. *In* The ecology of the seas. *Edited by* D.H. Cushing and J.J. Walsh. Blackwell Scientific Publications, Oxford, U.K. pp. 116–137.

Mangel, M., and Clark, C.W. 1988. Dynamic modelling in behavioral ecology. Princeton Univesity Press, Princeton, N.J.

Mauchline, J. 1960. The biology of the euphausiid crustacean, *Meganyctiphanes norvegica* Sars. Proc. R. Soc. Edinb. Sect. B (Biol.), **67**: 141–179.

McClatchie, S. 1985. Feeding behavior in *Meganyctiphanes norvegica* (M. Sars) (Crustaea: Euphausiacea). J. Exp. Mar. Biol. Ecol. **86**: 271–284.

McGurk, M.D. 1986. Natural mortality of marine pelagic fish eggs and larvae: role of spatial patchiness. Mar. Ecol. Prog. Ser. **34**: 227–242.

McLaren, I.A. 1963. Effects of temperature on growth of zooplankton and the adaptive value of vertical migration. J. Fish. Res. Board Can. **20**: 685–727.

Ohman, M.D. 1990. The demographic benefits of diel vertical migration by zooplankton. Ecol. Monogr. **60**: 257–281.

Omori, M., and Ikeda, T. 1984. Methods in marine zooplankton ecology. John Wiley & Sons, New York.

Onsrud, M.S.R., and Kaartvedt, S. 1998. Diel vertical migration of the krill *Meganyctiphanes norvegica* in relation to physics, food and predators. Mar. Ecol. Prog. Ser. **171**: 209–219.

Rosland, R., and Giske, J. 1994. A dynamic optimization model of the diel vertical distribution of a pelagic planktivorous fish. Prog. Oceanogr. **34**: 1–43.

Russell, F.S. 1927. The vertical distribution of plankton in the sea. Biol. Rev. Camb. Philos. Soc. **2**: 213–262.

Saborowski, R., Salomon, M., and Buchholz, F. 2000. The physiological response of krill (*Meganyctiphanes norvegica*) to temperature gradients in the Kattegat. Hydrobiologia, **426**: 157–160.

Stuart, V. 1986. Feeding and metabolism of *Euphausia lucens* in the southern Benguela current. Mar. Ecol. Prog. Ser. **30**: 117–125.

Tanasichuk, R.W. 1999. Euphausiids in a coastal upwelling ecosystem: their importance as fish prey, interannual variations in euphausiid population biology and productivity, and some implications of these changes for fish production. Ph.D. thesis, University of Bergen, Bergen, Norway.

Tarling, G.A., Matthews, J.B.L., David, P., Guerin-Ancy, O., and Buchholz, F. 1998*a*. Vertical migration and vertical velocities of zooplankton measured by an ADCP at the Ligurian Marine Front. *In* Fourth European Conference on Underwater Acoustics. *Edited by* A. Alippi and G.B. Cannelli. CNR-IDAC, Rome, Italy. pp. 235–240.

Tarling, G.A., Matthews, J.B.L., Sabarowski, R., and Buchholz, F. 1998*b*. Vertical migratory behaviour of the euphausiid *Meganyctiphanes norvegica*, and its dispersion in the Kattegat Channel. Hydrobiologia, **375/376**: 331–341.

Tarling, G.A., Buchholz, F., and Matthews, J.B.L. 1999. The effect of a lunar eclipse on the vertical migration of *Meganyctiphanes norvegica* (Crustacea: Euphausiacea) in the Ligurian Sea. J. Plankton Res. **21**: 1475–1488.

Winberg, G.G. 1971. Methods for the estimation of production of aquatic animals. Academic Press, London, U.K.

Zaret, M., and Suffern, J.S. 1976. Vertical migration in zooplankton as a predator avoidance mechanism. Limnol. Oceanogr. **21**: 804–812.